CHEMBIOCHEM

Supporting Information

Phosphine-activated Lysine Analogues for Fast Chemical Control of Protein Subcellular Localization and Protein SUMOylation

Joshua S. Wesalo, Ji Luo, Kunihiko Morihiro, Jihe Liu, and Alexander Deiters*

Department of Chemistry, University of Pittsburgh, Pittsburgh, PA 15260, USA

Table of Contents

1. Supporting Figures

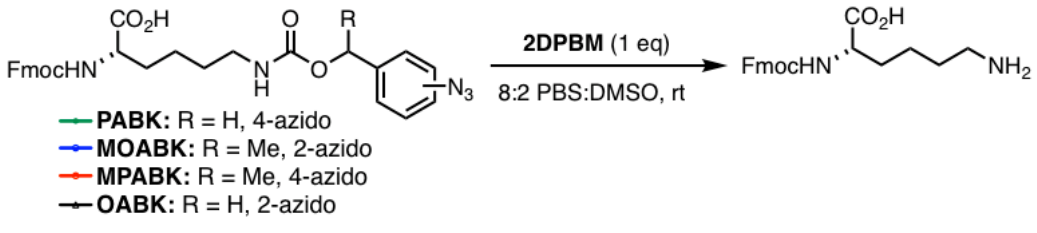

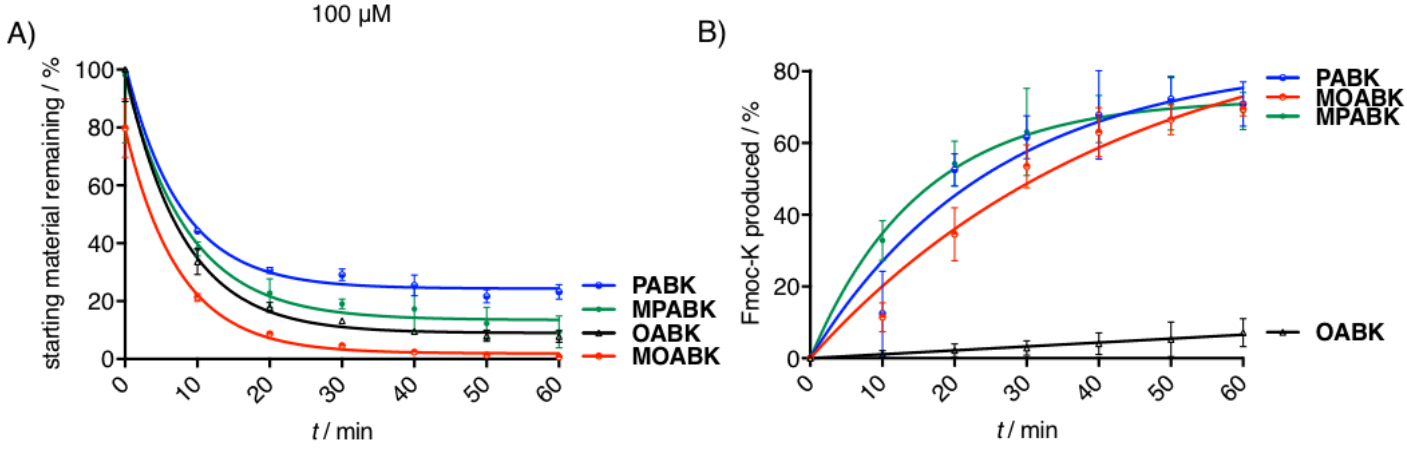

UAA	$t_{½}$ (min)	95% CI (min)	R^2
MPABK	6.0	3.7–9.0	0.92
PABK	5.3	3.3–7.9	0.92
MOABK	5.2	4.3–6.2	0.98
OABK	5.5	4.5–6.6	0.98

UAA	$t_{½}$ (min)	95% CI (min)	R^2
MPABK	10.5	7.9–14.1	0.94
PABK	17.7	11.4–31.1	0.90
MOABK	30.0	19.7–55.1	0.95
OABK	13972	very wide	0.48

Figure S1. A) LC-MS analysis of Fmoc-UAA (100 μM) consumption upon treatment with stoichiometric **2DPBM** in 8:2 PBS:DMSO; the rate is similar for all tested UAAs. **B**) Corresponding determination of Fmoc-K release under the same conditions by LC-MS. All three second-generation UAAs afforded approximately ten times the yield of Fmoc-K compared to **OABK**, and rates descended in the order **MPABK** > **PABK** > **MOABK** >> **OABK**. Reaction progress was monitored every 10 min. Mean ±SD (n = 3) is plotted.

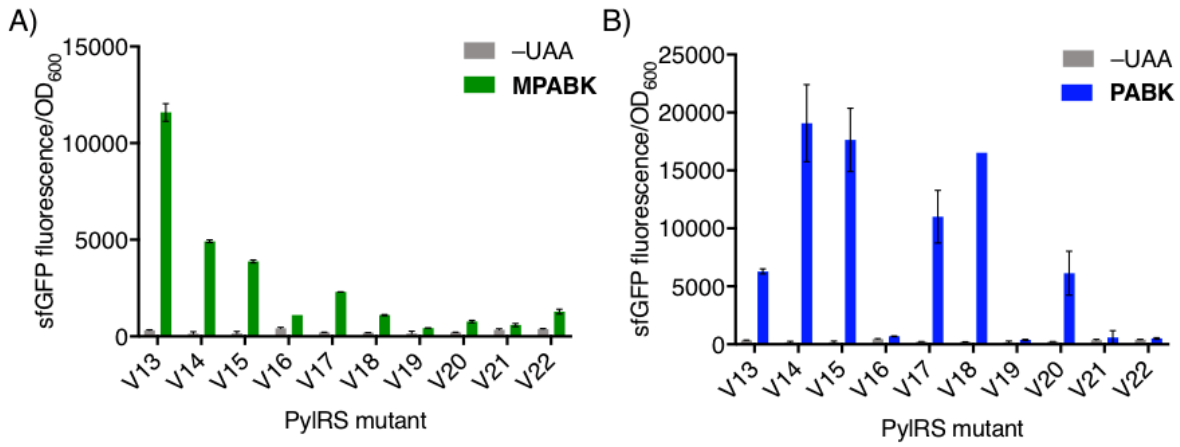

Figure S2. A) PylRS mutant screening for **MPABK** showed that V13 (Y271A-Y349F, previously reported as OABKRS)[1] gave the highest incorporation efficiency and negligible background signal in the absence of the UAA. **B**) Mutant screening for **PABK** showed that V14 (L274A-C313A-Y349F; PABKRS) incorporated **PABK** most efficiently. **PABK** is incorporated with much greater efficiency than **MPABK**. Mean ±SD (n = 2) is plotted. For V18 (**PABK**), the error bar is too small to be plotted.

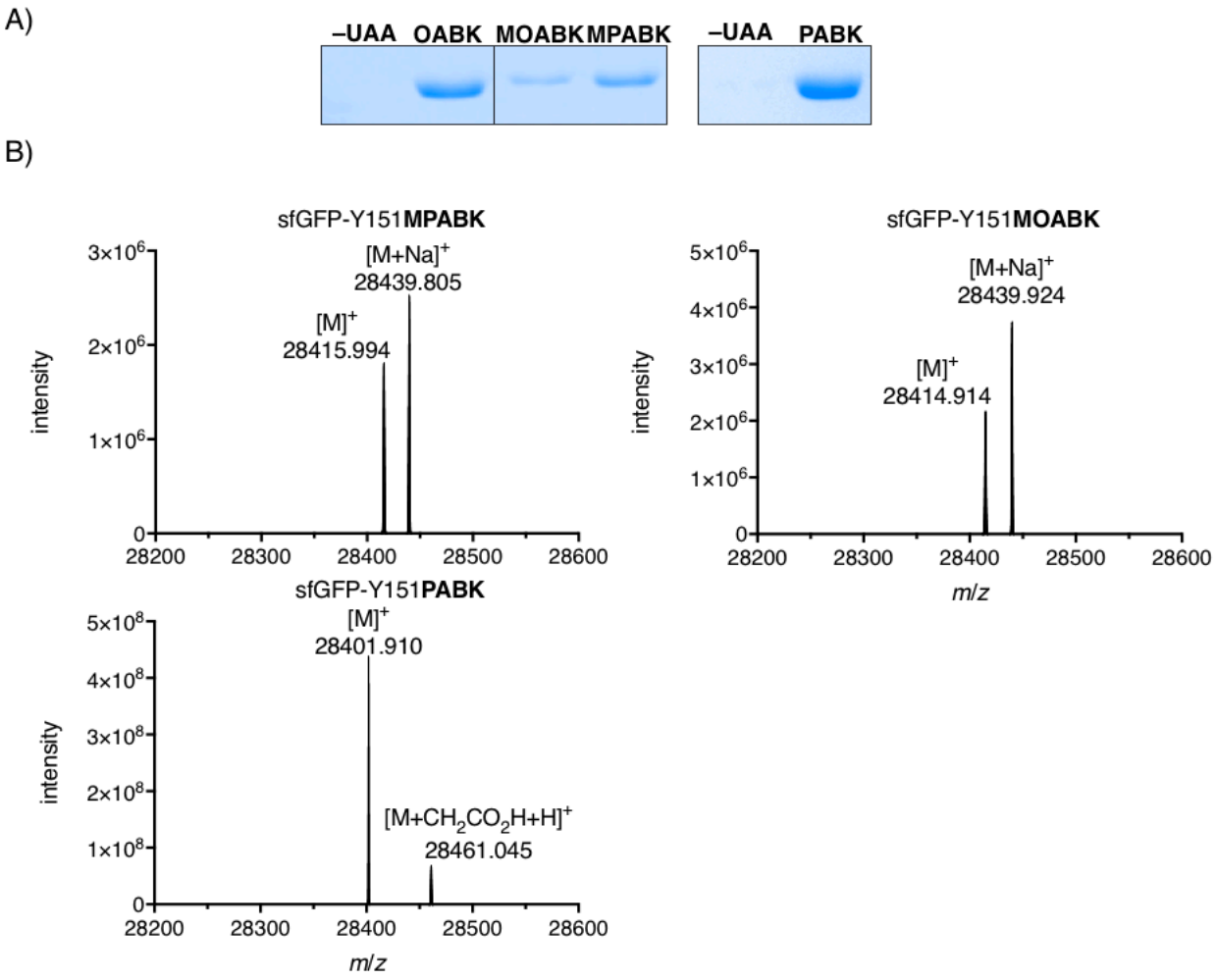

Figure S3. A) SDS-PAGE analysis of sfGFP mutants containing **OABK**, **MOABK**, **MPABK**, and **PABK** at position 151. Extra lanes analyzing lower-concentration elutions generated during the sfGFP-Y151**MPABK** purification were cropped between **OABK** and **MOABK** as indicated. No truncated protein was detected, which may be a result of instability or degradation of the N-terminal fragment. **B**) ESI-MS confirmation of sfGFP mutants containing **MOABK**, **MPABK**, and **PABK** at position 151. sfGFP-Y151**MPABK** ESI-MS (*m*/*z*) $[M]^+$ calculated for sfGFP-Y151**MPABK**: 28415.781; found 28415.994; $[M+Na]^+$ calculated for sfGFP-Y151**MPABK**: 28438.770; found 28439.805. ESI-MS (*m*/*z*) $[M]^+$ calculated for sfGFP-Y151**MOABK**: 28415.781; found 28414.914; $[M+Na]^+$ calculated for sfGFP-Y151**MOABK**: 28438.770; found 28439.924. ESI-MS (*m*/*z*) $[M]^+$ calculated for sfGFP-Y151**PABK**: 28401.765; found 28401.910. $[M+CH_2CO_2H+H]^+$ calculated for sfGFP-Y151**PABK**: 28460.778; found 28461.045. No reduction to the aniline[2,3] or decaging to lysine was observed.

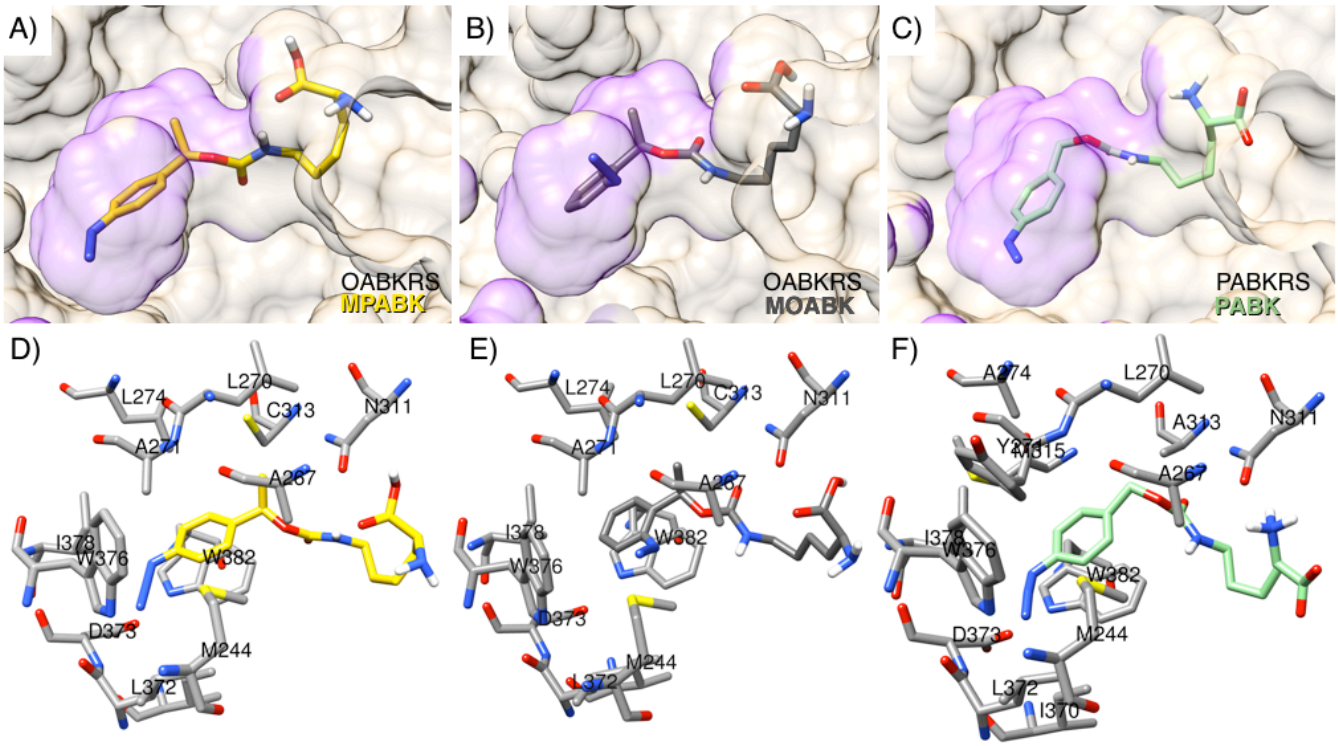

Figure S4. Docking studies of **MPABK** (**A** and **D**), **MOABK** (**B** and **E**), and **PABK** (**C** and **F**) into their respective synthetases. The lowest energy docked structures are shown within a surface representation of the catalytic pocket (top) and surrounded by the key side chain residues[4,5] thereof (bottom). **MPABK** and **PABK**, the more efficiently-incorporated UAAs, fit snugly into the distal pocket with the azide group projecting toward D373. This binding mode resembles that of N_ϵ-*meta*-azidobenzyloxycarbonyl-Lys.[6] For **MPABK** and **MOABK**, the benzylic methyl group projects upward into the tunnel and the α-carboxylate group is rotated away from ATP and toward N311. Thus, the α-carboxylate must rotate nearly 180° around the C_α–C_β bond to assume a catalytically-competent conformation as ween with Boc-Lys,[7] an exceptionally efficient PylRS substrate.[8,9] Structures were generated from PDB ID 4AAC.[6]

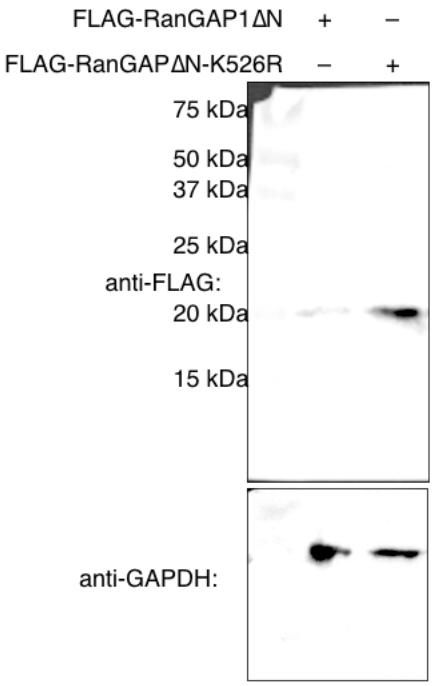

Figure S5. Western blot comparing FLAG-RanGAPΔN-K526R and WT FLAG-RanGAP1ΔN. Unmodified protein (~20 kDa) is only detected when the acceptor lysine K526 is mutated to R.

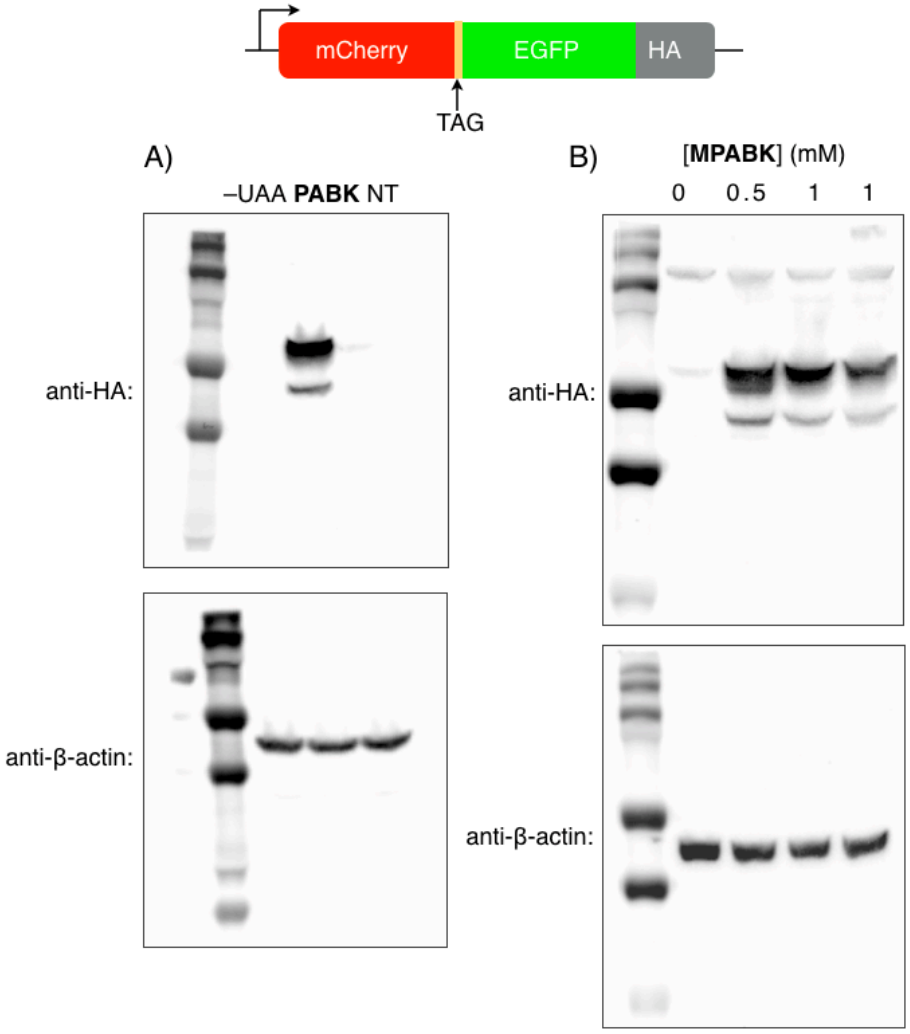

Figure S6. Full Western blots corresponding to **Figure 1.**

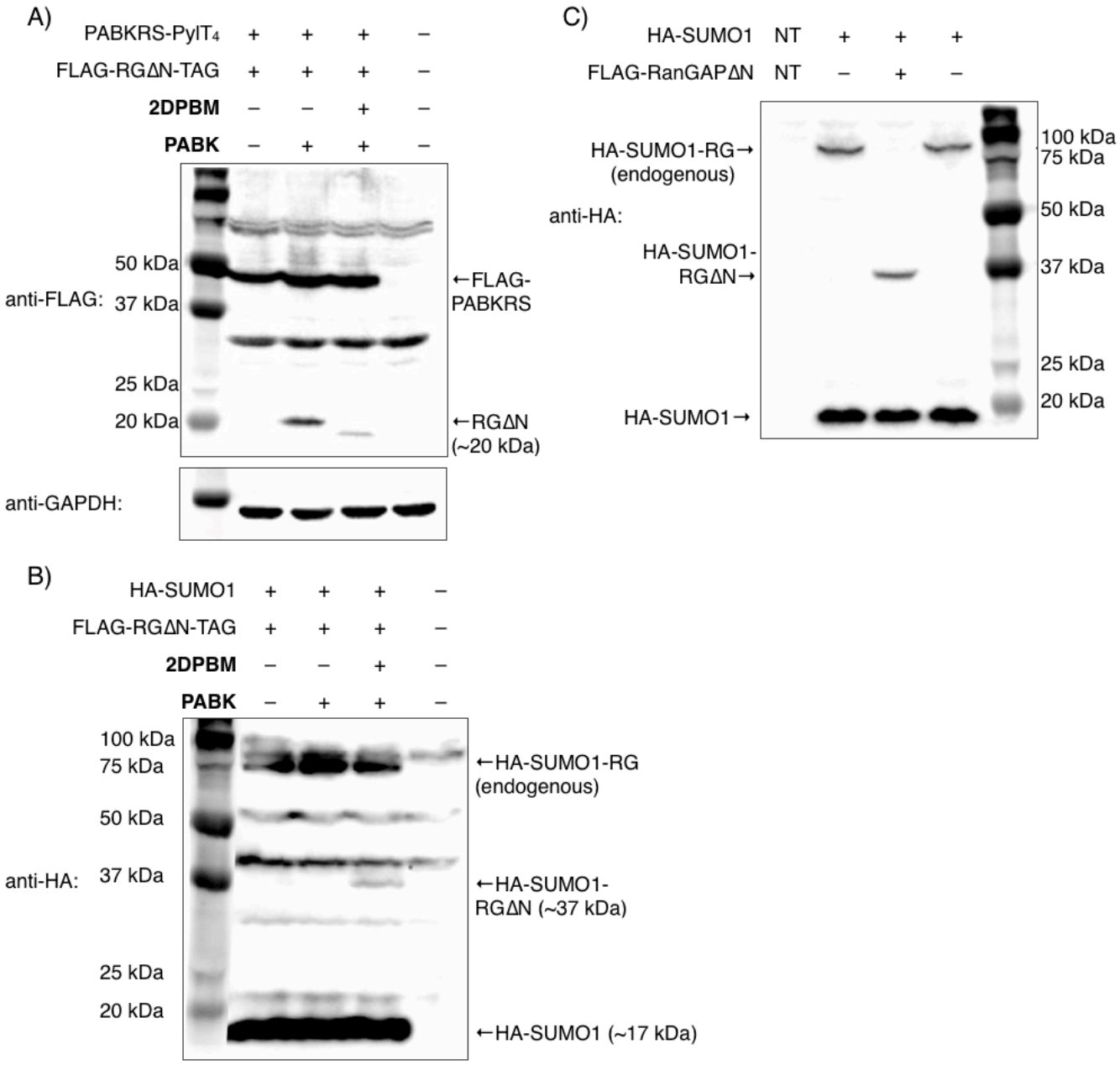

Figure S7. Full Western blots corresponding to **Figure 3**. **A**) Several nonspecific bands are visualized with the anti-FLAG antibody. **B**) Not surprisingly, several endogenous proteins conjugated with HA-SUMO1 are also seen with anti-HA antibodies (e.g., the band at ~22 kDa and endogenous SUMO1-RG). RG, RanGAP.

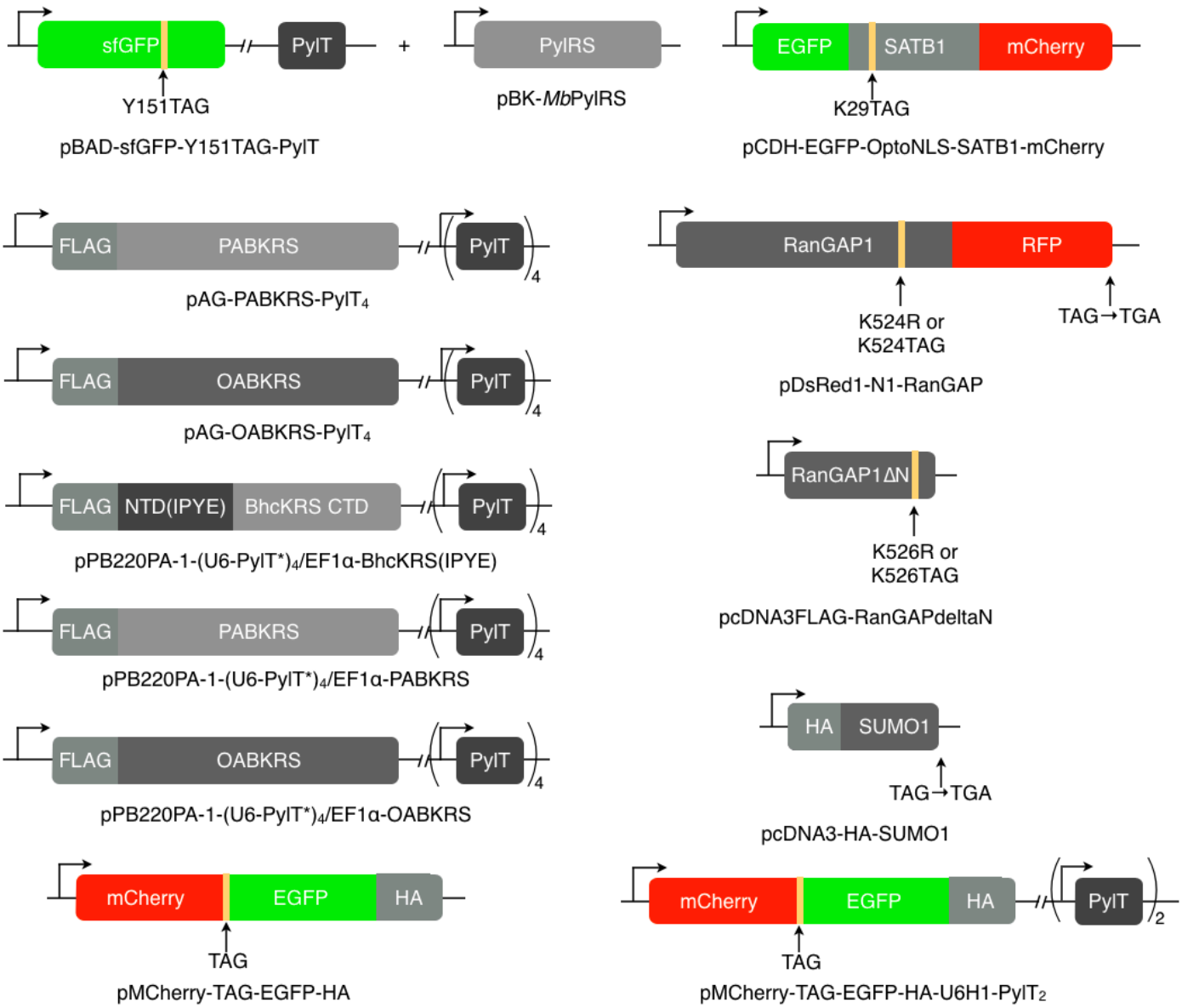

Figure S8. Maps of plasmids used in this work.

2. Supporting Note. Detection of SUMOylated RanGAP1ΔN.

SUMOylated FLAG-RanGAP1ΔN cannot be observed on anti-FLAG Western blots at the expected ~37 kDa apparent molecular weight.[10] FLAG tags' tyrosine residues may be differentially sulfated depending on expression conditions; sulfation prevents antibody recognition.[11] As SUMOylation affects other PTMs,[12] conditional tyrosine sulfation of SUMOylated FLAG-RanGAP1ΔN is plausible, and could be preventing antibody recognition. This can be circumvented with sulfatases, treatment with sodium chlorate,[11] or installation of multiple FLAG tags in tandem. On the other hand, FLAG-RanGAP1ΔN that is not modified with SUMO can be detected as a 20 kDa protein with an anti-FLAG antibody. As RanGAP1 SUMOylation is highly efficient,[13,14] we had to mutate the acceptor lysine to prevent SUMOylation using a K526R[15] (**Figure S5**) or K526**PABK** mutant (**Fig. 3b**) to observe the unmodified protein.

3. Supporting Methods

Biological protocols

HEK293T cells were obtained from American Type Culture Collection (ATCC, Manassas, VA) and were tested for contamination with *Mycoplasma spp.* every 3–6 months (MycoScope Mycoplasma PCR Detection Kit, Genlantis, San Diego, CA). All synthetase mutants were generated with the QuikChange II Site-Directed Mutagenesis kit (Agilent, Santa Clara, CA). pcDNA3flag-RanGAPdeltaN was a gift from Guy Salvesen (Addgene plasmid #25104; http://n2t.net/addgene:25104; RRID: Addgene_25104).[16] pcDNA3 HA-Sumo1 WT was a gift from Guy Salvesen (Addgene plasmid #48966; http://n2t.net/addgene:48966; RRID: Addgene_48966).[17] pDsRed1-N1 RanGAP was a gift from Mary Dasso (Addgene plasmid #13386; http://n2t.net/addgene:13386; RRID: Addgene_13386).[18] Phosphine stock solutions were prepared in DMSO degassed by sparging with argon for 30 min followed by 3 freeze-pump-thaw cycles, and were stored at –20 ºC in argon-flushed PCR tubes in an argon-flushed, parafilm-sealed 50 mL conical vial as 10 μL aliquots. Testing by ^{31}P-NMR (202 MHz, 4:1 DMSO-d_6:DMSO) demonstrated that **2DPBM** remains stable (<2% oxidation) after 5 months/5 freeze-thaw cycles, but as a precaution, a fresh aliquot was used for all experiments.

Incorporation of UAAs into proteins in *E. coli*. Chemically competent *E. coli* Top10 cells were co-transformed with the plasmids pBAD-sfGFP-Y151TAG-PylT[19] and pBK-*Mb*PylRS (several different mutants derived from pBK-JYRS from pBR322;[20] see **Table S2**). Cells were grown on lysogeny broth (LB)-agar plates containing kanamycin (50 μg mL^{-1}) and tetracycline (25 μg mL^{-1}) as selection agents. A 2 mL starter culture of LB containing these antibiotics was inoculated with a single colony from the plate. Saturated overnight starter cultures were diluted 1:50 into 200 μL LB supplemented with the antibiotics on deep well 96-well plates for synthetase screening. The cultures were grown at 37 ºC, 250 rpm, for ca. 6 hours until A_{600} reached 0.5–0.6. At this point, UAAs were added as 100 mM stock solutions in DMSO to a final concentration of 1 mM, and expression was induced with arabinose (0.2% (w/v)). After overnight expression, the suspension (100 μL) was transferred to a black 96-well plate for fluorescence readouts (synthetase screening). Fluorescence (λ_{ex} = 488 nm, λ_{em} = 510 nm) and A_{600} was read on an Infinite M1000Pro plate reader (Tecan, Zürich, Switzerland). For bulk protein expressions, saturated overnight cultures were diluted 1:100 into 5 mL or 20 mL LB cultures containing the appropriate antibiotics. After induction with arabinose (0.2% (w/v)) at A_{600} 0.5–0.6 and overnight growth, cultures were pelleted to obtain purified protein for characterization by SDS-PAGE and ESI-MS. Pellets were resuspended in 5 mL lysis buffer (50 mM sodium phosphate, pH 8.0), to which 50 μL protease inhibitor cocktail and 50 μL of lysozyme (100 mg mL^{-1}) in water was added. The suspensions were gently mixed by inverting them several times, and were incubated on ice for 90 minutes. They were then sonicated on ice (10 seconds on, 10 seconds off for 4 minutes), and were centrifuged at 13,000 g, 4 ºC for 20 minutes. The supernatants were transferred to centrifuge tubes, mixed with 75 μL of Ni-NTA resin (Qiagen, Hilden, Germany), and incubated while rocking for 2 hours on ice. Afterwards, the resin was pelleted (500 g, 10 minutes). The pellet was washed by gently resuspending it in lysis buffer containing 10 mM imidazole (3 x 500 μL), followed by lysis buffer containing 30 mM imidazole (2 x 500 μL). Resin was pelleted by centrifugation for 1 minute at 800 g between each wash. The protein was eluted with 3 x 75 μL lysis buffer (250 mM imidazole), and was analyzed by SDS-PAGE (stained with Coomassie Brilliant Blue G and imaged with a ChemiDoc XRS+ system (Bio-Rad, Hercules, CA) and by ESI-MS as described below (see **mass spectrometry analysis of proteins**). Protein yields were quantified densitometrically in Image Lab 6.0 (Bio-Rad, Hercules, CA) using a three-point bovine serum albumin (Thermo Scientific, Rockford, IL) standard curve run on each gel.

Quantification of fluorescence measurements. Fluorescence intensity was quantified using Fiji.[21,22] Raw image files for the mCherry, EGFP, and brightfield channels were stacked in chronological order and saved as .tif files. Stacks were viewed synchronously so that the EGFP channel could be used to delineate cell borders while mCherry was quantified. Oval areas representative of the nucleus and cytosol were measured (both average and median intensity) for 3 representative cells at each time point. Additionally, a background measurement in an area with no cells present was recorded. Data were transferred to Microsoft Excel 15.27 (Microsoft, Redmond, WA). The background signal was subtracted; in the rare event that the background-

corrected intensity value was negative, the data point was set to 0 as reported previously.[23] $\frac{I_n}{I_n+I_c}$ was calculated for each cell at each time point (values were nearly identical for mean and median intensity values, and mean was used for the analysis; I_n = nuclear intensity, I_c = cytosolic intensity). For **Figure 2c**, each datum e_i was scaled from 0 to 1 by taking $Scaled\ (e_i) = \frac{e_i - E_{min}}{E_{max} - E_{min}}$. Averages and standard deviations were then calculated for the 3 cells. Data were plotted in GraphPad Prism 7 (GraphPad Software, San Diego, CA) and modeled as a four-parameter logistic curve functions with the baseline data point excluded (since the time point 5 minutes before phosphine treatment is meaningless for modeling nuclear translocation kinetics). The modeled curves were used to determine $t_{½}$. The bottom parameter was constrained to 0.24 for the 25 μM and 10 μM **2DPBM** treatments of **PABK**.

Mass spectrometry analysis of proteins. High-resolution (≥ 10,000 R FWHM) mass spectrometry of sfGFP-Y151**MPABK**, sfGFP-Y151**MOABK**, and sfGFP-Y151**PABK** was carried out using electrospray ionization (ESI) on a Thermo Scientific Q-Exactive Orbitrap mass spectrometer (Bremen, Germany) connected to a Dionex Ultimate 3000 UHPLC system. The sample was analyzed through a ProSwift RP-10R 1 mm x 5 cm column, flow rate 200 µL min^{-1} and ACN gradient (0.1% formic acid) 26→80% for 30 min. The mass spectrometer was operated in positive-ion mode with a capillary voltage of 3.5 kV and resolution at 17,500. Sheath gas, aux gas, and sweep gas flow rates were 35, 10, and 5, respectively. Source temperature was 250 °C. The S-lens RF level voltage was 50 V and the ion transfer tube temperature was 250 °C. The instrument was tuned and calibrated with Pierce LTQ ESI positive ion calibration solution (Thermo Scientific, Waltham, MA) and the data were collected for *m/z* values ranging from 500-3000. Xcalibur 3.0.63 and Protein Deconvolution 3.0 software was used for the data analysis.

LC-MS analysis of UAA deprotection with 2DPBM. Time course extracted ion chromatograms were obtained from LC-ESI-MS analysis of the reaction of Fmoc-protected UAAs (0.1 mM) with **2DPBM** (1 equiv.) in PBS buffer (pH 7.4):DMSO = 9:1 (**Figure S1**). The reaction mixture was analyzed at different time points using a Hypersil GOLD C18 column, 1.9 um, 2.1 mm i.d. x 100 mm (Thermo Scientific, Waltham, MA) on a Prominence HPLC system (Shimadzu, Kyoto, Japan). The LC system was directly coupled to an electrospray ionization mass spectrometer (LCMS-2020, Shimadzu). LC gradient = 5-60% MeCN in 0.1% aqueous formic acid, flow rate = 0.2 mL min^{-1}, column temperature = 40 °C.

Modeling of UAAs in PylRS mutant active sites. The crystal structure for the *Methanosarcina mazei* homolog of OABKRS's C-terminal domain (CTD) in complex with *meta*-azido-*N*$^{\epsilon}$-Cbz-Lys[6] was used directly for modeling **MPABK** and **MOABK** (PDB ID: 6AAC). For **PABK**, PABKRS's CTD was modeled by making the A306Y, L309A, and C348A mutations based on the Dunbrack 2010 rotamer library[24] in UCSF Chimera[25] v1.13.1. All residues containing atoms clashing with their van der Waals radii overlapping by ≥0.6 Å as a result of the A306Y mutation were energy minimized with 2 rounds of 1,500 0.02 Å steepest descent steps and 30 0.02 Å conjugate gradient steps. UAA 3D structures were generated and energy-minimized to an RMS gradient of 0.01 in Chem3D v16.0.1.4 (Perkin Elmer, Waltham, MA) using the MM2 method. UAA structures were imported into Chimera. Structures were prepared for binding by assigning charges using ANTECHAMBER with the Gasteiger method.[26] UAAs were docked into the catalytic pocket using AutoDock Vina[27] v1.1.2 (10 binding modes, maximum search exhaustiveness, 3 kcal/mol maximum energy difference). Molecular surfaces were calculated and rendered in Chimera using the MSMS package.[28] To generate the cartoon SATB1 NLS in **Figure 2**, thirty models of the SATB1 NLS sequence (VSDPKGPPAKIARLEQNGSPL)[29] were computed in Chimera using Modeller[30] with the DOPE-HR modeling protocol,[31] and the model with the highest GA341 score and lowest zDOPE value was selected.

Plasmid construction for mammalian cell applications.

Note: all transgenes ending in a TAG stop codon were mutated to TGA before use (HA-SUMO1 and RanGAP1-RFP).

1. pAG-*Mb*PylOABKRS-PylT$_4$ was reported by our group previously[1] and was mutated to PABKRS using a QuikChange II site-directed mutagenesis kit (Agilent, Santa Clara, CA) with primers P1–P4.
2. RanGAP and SUMO1 plasmids were obtained from Addgene as described in **Biological experiments**. Mutations with primers P5–P16 were made using a QuikChange II site-directed mutagenesis kit (Agilent, Santa Clara, CA).
3. pPB220PA-1-(U6-PylT*)$_4$/EF1α-BhcKRS(IPYE) was assembled via three-fragment Gibson assembly.[32] The backbone, pPB220PA-1-(U6-PylT*)$_4$/EF1α-PylRS, was obtained from Jason Chin (Medical Research Council Laboratory of Molecular Biology, Cambridge, UK). The Y217A and L274M mutations for BhcKRS[19] were made in a single reaction using a QuikChange II site-directed mutagenesis kit (Agilent, Santa Clara, CA) and primers P17 and P18. To create the improved chimeric[33,34] version, three fragments were used:
    i. The backbone was prepared by digesting pPB220PA-1-(U6-PylT*)$_4$/EF1α-PylRS with NotI-HF and PmeI (37 ºC, 6 h, CutSmart Buffer, 4 μg DNA and 1.25 μL each enzyme, New England BioLabs, Ipswich, MA). The 8,602 bp fragment was purified by extraction from a 0.8% TBE-agarose gel (E.Z.N.A. Gel Extraction Kit, Omega Bio-Tek, Norcross, GA).
    ii. The N-terminal domain (NTD) containing the V30I, T56P, H62Y, and A100E mutations[34] was amplified with P19 and P20 from a gene fragment ordered from Twist Biosciences (San Francisco, CA). The gene fragment sequence is as follows (adapter sequences added by the manufacturer are bolded and underlined):

    GAAGTGCCATTCCGCCTGACCTCATGGACTACAAGGACGACGACGACAAGGACAA
    GAAGCCTTTGGATGTACTCATAAGTGCCACTGGTCTCTGGATGTCACGGACCGGAA
    CGCTCCATAAAATCAAACATTACGAAATCTCCCGCTCCAAAATCTACATTGAGATGG
    CATGTGGGGACCATCTGGTTGTAAATAACTCTCGGAGCTGCAGGCCAGCGCGGGC
    CTTCAGATATCATAAATATCGCAAGACATGCAAGCGATGCCGCGTGTCTGATGAGG
    ACATAAACAATTTTCTGACCAGATCAACAGAGGGTAAGACAAGCGTGAAAGTCAAA
    GTGGTTAGCGAGCCAAAGGTAAAAAAGGCCATGCCCAAATCTGTGTCTCGGGCAC
    CTAAGCCGCTCGAAAACCCTGTGTCCGCGAAAGCGAGCACGGATACGTCACGCTC
    CGTACCGTCTCCGGCTAAGAGTACGCCCAATTCCCCCGTTCCAACATCTGCCTCTG
    CCCCAGCCCTGAC**AGGCTAGGTGGAGGCTCAGTG**

    The gene fragment was amplified by PCR with P19 and P20 using Phusion polymerase (Thermo Scientific, Waltham, MA). The PCR product was purified using an E.Z.N.A. Cycle Pure Kit (Omega Bio-Tek, Norcross, GA).

    iii. The C-terminal domain was amplified from pPB220PA-1-(U6-PylT*)$_4$/EF1α-BhcKRS using P21 and P22. The template DNA was digested with DpnI (New England BioLabs, Ipswitch, MA) overnight. The PCR product was purified using an E.Z.N.A. Cycle Pure Kit (Omega Bio-Tek, Norcross, GA).

    The fragments (4.25 eq per equivalent of backbone, 100 ng total) were assembled by isothermal Gibson assembly.[32] The DNA was added as a 5 μL solution to a 15 μL portion of 1.33x isothermal Gibson assembly master mix[32] on ice, and the reaction mixture was incubated at 50 ºC for 1 h. The product was transformed into chemically-competent Top10 cells. Insert sequences were confirmed by Sanger sequencing (Genewiz, South Plainfield, NJ).

4. pMCherry-TAG-EGFP-HA-U6H1-PylT$_2$ was assembled by cloning the U6H1-PylT$_2$ cassette,[35] which was ordered as a gBlock (Integrated DNA Technologies, Coralville, IA), into pMCherry-

TAG-EGFP-HA using the MfeI and MluI restriction sites and T4 ligase (16 ºC, overnight). The gBlock sequence was as follows. Restriction sites are capitalized. The *Desulfitobacterium hafniense* PylT gene is labeled in blue, and the *M. barkeri* homolog in red:

ggtaggCAATTGaaggtcgggcaggaagagggcctatttcccatgattccttcatatttgcatatacgatacaaggctgttagaga
gataattagaattaatttgactgtaaacacaaagatattagtacaaaatacgtgacgtagaaagtaataatttcttgggtagtttgcagttt
taaaattatgttttaaaatggactatcatatgcttaccgtaacttgaaagtatttcgatttcttggctttatatatcttgtggaaaggacgggg
ggtggatcgaatagatcacacggactctaaattcgtgcaggcgggtgaaactcccgtactccccgttttttggatctgacaagtgcggtt
tttgctagtcaattcgaacgctgacgtcatcaacccgctccaaggaatcgcgggcccagtgtcactaggcgggaacacccagcgcg
cgtgcgccctggcaggaagatggctgtgagggacaggggagtggcgccctgcaatatttgcatgtcgctatgtgttctgggaaatca
ccataaacgtgaaatgtctttggatttgggaatcttataagttctgtatgagaccacagctctggaacctgatcatgtagatcgaacgg
actctaaatccgttcagccgggttagattcccggggtttccgttttttggatctAGATCTttatcg

5. pPB220PA-1-(U6-PylT*)$_4$/EF1α-OABKRS and pPB220PA-1-(U6-PylT*)$_4$/EF1α-PABKRS were by Gibson assembly.
    i. The synthetases were amplified from pAG-OABKRS-PylT$_4$ and pAG-PABKRS-PylT$_4$ with primers P23 and P24. The template DNA was digested with DpnI (New England BioLabs, Ipswitch, MA) overnight. The PCR product was purified using an E.Z.N.A. Cycle Pure Kit (Omega Bio-Tek, Norcross, GA).

    ii. The backbone was prepared in 3.i above.

    The PylRS fragment (3.5 eq per equivalent of backbone or 53 ng) and backbone (100 ng) were assembled by isothermal Gibson assembly.[32] The DNA was added as a 5 μL solution to a 15 μL portion of 1.33x isothermal Gibson assembly master mix[32] on ice, and the reaction mixture was incubated at 50 ºC for 1 h. The product was transformed by electroporation into Top10 cells. Insert sequences were confirmed by Sanger sequencing.

Table S1. Primer sequences (5' to 3') used in this work. All primers were purchased from Sigma-Aldrich (St. Louis, MO). In P1–P18, mutated codons are indicated in lowercase. In P19, P23, and P24, lowercase is used to indicate the portions of the primer corresponding to the backbone (vector), and uppercase shows the sequence of PylRS. For P5 and P6, x = 6 for the murine homolog (used for Western blot), and x = 4 (used for imaging as the dsRed fusion protein).

ID	Gene	Purpose	Sequence
P1	PABKRS	C313A mutation	GAA TTC ACC ATG GTT AAC TTT gcg CAA ATG GGC AGC GGC TG
P2	PABKRS	C313A mutation	CAG CCG CTG CCC ATT TGc gcA AAG TTA ACC ATG GTG AAT TC
P3	PABKRS	L274A mutation	GCT GGC CCC CAC CCT GTA CAA CTA Cgc cCG GAA ACT GGA CAG AAT C
P4	PABKRS	L274A mutation	GAT TCT GTC CAG TTT CCG ggc GTA GTT GTA CAG GGT GGG GGC CAG C
P5	RanGAP	K52xR mutation	GTG CAC ATG GGT CTG CTC agg AGT GAA GAC AAG GTC AAG
P6	RanGAP	K52xR mutation	CTT GAC CTT GTC TTC ACT cct GAG CAG ACC CAT GTG CAC
P7	RanGAP (mouse)	K526TAG mutation	GGG TCT GCT Cta gAG TGA AGA CAA GGT CAA GGC
P8	RanGAP (mouse)	K526TAG mutation	GTC TTC ACT cta GAG CAG ACC CAT GTG CAC GAG
P9	RanGAP (mouse)	TAG590TGA mutation	GTA CAA GGT Ctg aCT CGA GCA TGC ATC TAG AGG
P10	RanGAP (mouse)	TAG590TGA mutation	ATG CTC GAG tca GAC CTT GTA CAG CGT CTG C
P11	RanGAP (human)	K524TAG mutation	GTG CAC ATG GGT CTG CTC tag AGT GAA GAC AAG GTC AAG
P12	RanGAP (human)	K524TAG mutation	CTT GAC CTT GTC TTC ACT cta GAG CAG ACC CAT GTG CAC
P13	SUMO1	TAG109TGA mutation	CAG GAA CAA ACG GGG GGT tga CTC GAG CAT GCA TCT AG
P14	SUMO1	TAG109TGA mutation	CTA GAT GCA TGC TCG AGt caA CCC CCC GTTTGTTCCTG
P15	dsRed	TAG227TGA mutation	CTG TTC CTG tga CGG CCG CGA CTC TAG ATC AT
P16	dsRed	TAG227TGA mutation	GTC GCG GCC Gtc aCA GGA ACA GGT GGT
P17	BhcKRS	Y271A and L274M mutations	CCT ATG CTG GCC CCC ACC CTG gcc AAC TAC atg CGG AAA CTG GAC AGA ATC
P18	BhcKRS	Y271A and L274M mutations	GGA TTC TGT CCA GTT TCC Gca tGT AGT Tgg cCA GGG TGG GGG CCA GCA TAG G
P19	PylRS-NTD(IPYE)	Gibson assembly	gac cgg cgc cta ctc tag agc tag cgt tta aac tta agc ttg cca cCA TGG ACT ACA AGG ACG ACG ACG AC
P20	PylRS-NTD(IPYE)	Gibson assembly	GTC AGG GCT GGG GCA GAG GC
P21	PylRS-CTD	Gibson assembly	CCC CTG TGC AGG CCT CTG CCC CAG CCC TGA C
P22	PylRS-CTD	Gibson assembly	CAA GCG GCT TCG GCC AGT AAC
P23	PylRS	Gibson assembly	gct gtg acc ggc gcc tac tct aga gct agc gtt taa act taa gct tgc cac cAT GGA CTA CAA GGA CGA CGA CG
P24	PylRS	Gibson assembly	cgt tag ggg ggg ggg agg gag agg ggc gcg gcc gct gTC ATC ACA GGT TGG TGC TGA TG

Synthetic protocols

General synthetic procedures. Reactions were monitored by thin layer chromatography (TLC) using glass-backed silica gel HL (F254, Sorbtech, 250 µm thickness). All reagents and solvents obtained from commercial suppliers were used without further purification. Reactions using anhydrous solvents were performed in flame-dried glassware under a nitrogen atmosphere. Yields refer to chromatographically- and spectroscopically-pure compounds. Flash chromatography was performed with silica gel (Sorbtech, 60 Å, 230–400 mesh) as a stationary phase according to the method of Still, Kahn, and Mitra[36] or on a CombiFlash Rf system (TeleDyne ISCO, Lincoln, NE) using commercial silica gel cartridges (Agela, Torrance, CA).

^{1}H- and ^{13}C-nuclear magnetic resonance (NMR) spectra were obtained on 300 MHz, 400 MHz, 500 MHz, or 600 MHz Bruker NMR spectrometers, and chemical shifts are in δ units (ppm) relative to the solvent signal.[37] Electrospray ionization (ESI) mass spectra were obtained using a Q Exactive Hybrid Quadrupole-Orbitrap mass spectrometer (Thermo Scientific) or a Q-TOF Ultima API mass spectrometer (Micromass UK Limited).

2-(Diphenylphosphino)benzamide (**2DPBM**) was prepared according to published procedures.[38]

Synthesis of PABK. Diazotization of commercially-available 4-aminobenzyl alcohol **1** gave 4-azidobenzyl alcohol **2** in high yield. Treatment with *N,N'*-disuccinimidyl carbonate (DSC) in MeCN in the presence of trimethylamine (Et_3N) afforded a moderate yield of NHS carbonate **3**. Displacement with N^{α}-Fmoc-Lys-OH in DMF furnished Fmoc-**PABK 4** in good yield (improving on known route[39] by increasing yield and making purification easier). Subsequent deprotection with piperidine in dichloromethane followed by acidification with HCl and precipitation in ether furnished **PABK 5**, albeit in modest yield (**Scheme S1**).

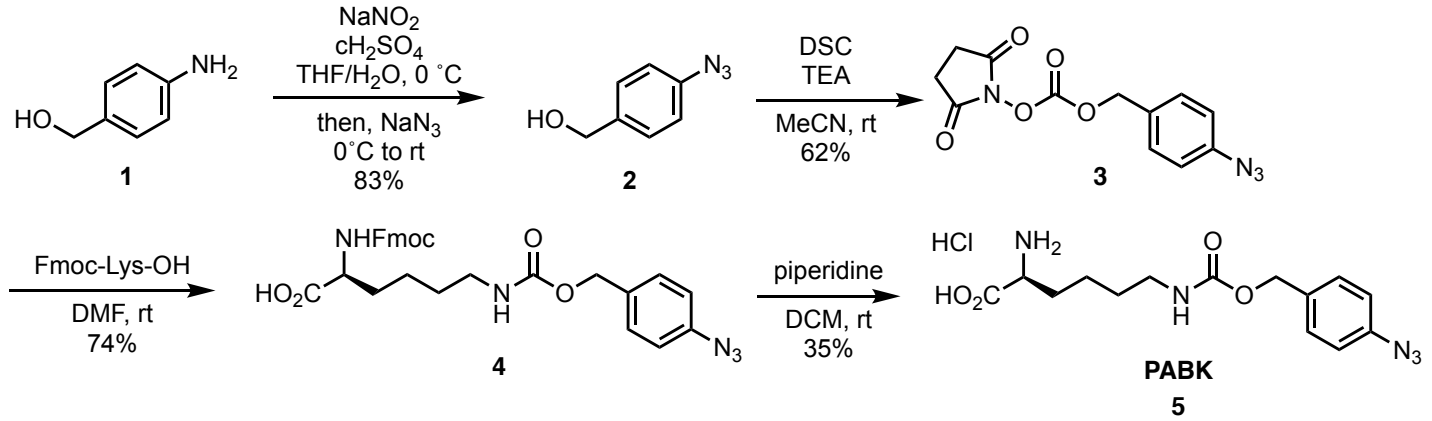

Scheme S1. Synthesis of **PABK** in four steps from 4-aminobenzyl alcohol.

4-Azidobenzyl alcohol (2). 4-Aminobenzyl alcohol (**1**) (800 mg, 6.50 mmol) was dissolved in THF (9.6 mL) and H_2O (28 mL) and conc. H_2SO_4 (2.2 mL) and $NaNO_2$ (556 mg, 8.05 mmol) in H_2O (4.7 mL) were added at 0 ˚C. The reaction mixture was stirred at 0 ˚C for 1 h and NaN_3 (523 mg, 8.05 mmol) in H_2O (2.3 mL) was added. The reaction mixture was stirred for 1 h at rt and diluted with DCM. The organic layer was washed with brine and dried over Na_2SO_4. The solvent was removed *in vacuo* and the residue was purified by flash chromatography over silica gel, eluting with hexanes/EtOAc (4:1) to give compound **2** (800 mg, 83%) as a yellow oil. The analytical data matched reported results.[40]

4-Azidobenzyl (2,5-dioxopyrrolidin-1-yl) carbonate (3). Compound **2** (150 mg, 1.00 mmol) was dissolved in MeCN (10 mL) and DSC (512 mg, 2.00 mmol) and TEA (0.42 mL, 3.00 mmol) were added at room temperature. The reaction mixture was stirred at room temperature for 4 h and the solvent was removed *in vacuo*. The residue was purified by flash chromatography on silica gel, eluting with hexanes/EtOAc (7:3) to give compound **3** (180 mg, 62%) as a yellow solid. ^{1}H NMR (300 MHz, $CDCl_3$): δ = 7.44-7.47 (d, *J* = 8.4 Hz, 2H), 6.99-7.02 (d, *J* = 8.4

Hz, 2H), 5.05 (s, 2H), 2.64 (s, 4H). ^{13}C NMR (400 MHz, $CDCl_3$): δ = 25.6, 78.1, 119.3, 130.2, 131.8, 141.4, 150.1, 171.4. HRMS data could not be obtained due to the instability of this compound.

***N*^{2}-(((9*H*-Fluoren-9-yl)methoxy)carbonyl)-*N*^{6}-(((4-azidobenzyl)oxy)carbonyl)-*L*-lysine (Fmoc-PABK, 4).** Compound **117** (180 mg, 0.621 mmol) was dissolved in DMF (6.2 mL) and Fmoc-Lys-OH (274mg, 0.745 mmol) was added at room temperature. The reaction mixture was stirred at room temperature for 3 h and diluted with Et_2O. The solution was washed with H_2O and brine and the organic layer was dried over Na_2SO_4. The solvent was removed *in vacuo* and the residue was purified by flash chromatography on silica gel, eluting with DCM/MeOH (9:1) to give compound **4** (250 mg, 74%) as a white solid. The analytical data matched reported results.[39]

***N*^{6}-(((4-Azidobenzyl)oxy)carbonyl)-*L*-lysine hydrochloride salt (PABK, 5).** Compound **118** (20 mg, 0.368 μmol) was dissolved in DCM (3.2 mL) and piperidine (0.55 mL) was added at room temperature. The reaction mixture was stirred at room temperature for 2 h and the solvent was removed *in vacuo*. The residue was purified by flash chromatography on silica gel, eluting with DCM/MeOH (1:1). The solvent was removed *in vacuo* and the residue was dissolved in MeOH (1.0 mL) containing conc. HCl (aq.) (10 μL) and dropped into Et_2O. The resulting solid was washed with MeCN to give compound **5** (41 mg, 35%) as a pale yellow solid. The analytical data matched reported results.[39]

Preparation of MOABK. Commercially-available 2-aminoacetophenone **6** was diazotized and treated with sodium azide to give 2-azidoacetophenone **7** in moderate yield. Reduction with sodium borohydride in methanol cleanly reduced **7** to alcohol **8** in near-quantitative yield. Treatment with DSC in MeCN in the presence of Et_3N gave NHS carbonate **9** in excellent yield. Treatment with *N*^{α}-Fmoc-Lys-OH in DMF gave Fmoc-**MOABK 10** in good yield, and deprotection with piperidine furnished **MOABK 11** in moderate yield (**Scheme S2**).

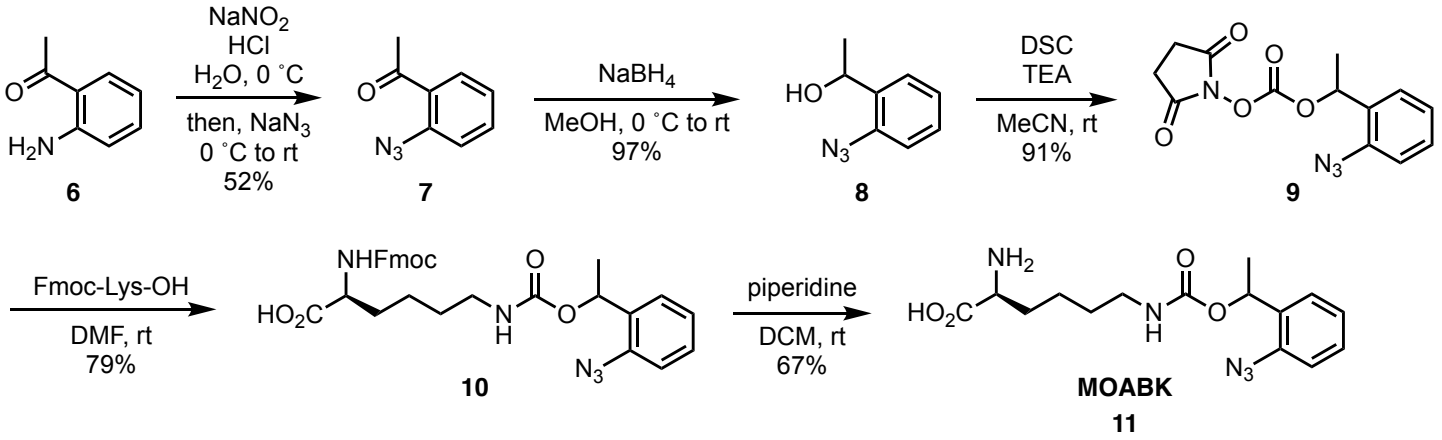

Scheme S2. Synthesis of **MOABK** in 5 steps from 2-aminoacetophenone.

2-Azidoacetophenone (7). 2-Aminoacetophanone (**6**) (0.9 mL, 7.40 mmol) was dissolved in 5 M HCl (aq.) (16 mL) and $NaNO_2$ (613 mg, 8.88 mmol) was added at 0 °C. The reaction mixture was stirred at 0 °C for 0.5 h, then NaN_3 (577 mg, 8.88 mmol) was added over 1 h. The reaction mixture was stirred at room temperature for 2 h and extracted by EtOAc. The organic layer was washed with brine and dried over Na_2SO_4. The solvent was removed *in vacuo* and the residue was purified by flash chromatography on silica gel, eluting with hexanes/EtOAc (9:1) to give compound **7** (618 mg, 52%) as a yellow oil. The analytical data matched reported results.[41]

1-(2-Azidophenyl)ethane-1-ol (8). Compound **7** (610 mg, 3.79 mmol) was dissolved in MeOH (15 mL) and $NaBH_4$ (143 mg, 3.79 mmol) was added at 0 °C. The reaction mixture was stirred at room temperature for 1 h and the solvent was removed in vacuo. The residue was diluted with EtOAc and washed with H_2O and brine. The organic layer was dried over Na_2SO_4 and the solvent was removed *in vacuo*. The residue was purified by flash chromatography on silica gel, eluting with hexanes/EtOAc (9:1) to give compound **8** (598 mg, 97%) as a yellow oil. The analytical data matched reported results.[42]

1-(2-Azidophenyl)ethane-(2,5-dioxopyrrolidin-1-yl) carbonate (9). Compound **8** (408 mg, 2.50 mmol) was dissolved in MeCN (10 mL) and DSC (1.28 g, 5.00 mmol) and TEA (1.0 mL, 7.50 mmol) were added at room temperature. The reaction mixture was stirred at room temperature for 6 h and the solvent was removed *in vacuo*. The residue was purified by flash chromatography on silica gel, eluting with hexanes/EtOAc (9:1 to 1:1) to give compound **9** (690 mg, 91%) as a pale yellow solid. ^{1}H NMR (400 MHz, $CDCl_3$) δ = 7.46 (dd, *J* = 8 and 1 Hz, 1H), 7.38 (dt, *J* = 8 and 1 Hz, 1H), 7.22-7.16 (m, 2H), 6.08 (dd, *J* = 13 and 7 Hz, 1H), 2.81 (s, 4H), 1.63 (d, *J* = 7 Hz, 3H); ^{13}C NMR (100 MHz, $CDCl_3$) δ = 168.6, 150.8, 136.8, 130.6, 129.7, 126.3, 125.2, 118.1, 75.6, 25.3, 21.0. HRMS data could not be obtained due to instability of this compound.

***N*^{2}-(((9*H*-Fluoren-9-yl)methoxy)carbonyl)-*N*^{6}-((1-(2-azidophenyl)ethoxy)carbonyl)-*L*-lysine (Fmoc-MOABK**, **10).** Compound **9** (200 mg, 0.658 mmol) was dissolved in DMF (6.6 mL) and Fmoc-Lys-OH (291 mg, 0.790 mmol) was added at room temperature. The reaction mixture was stirred at room temperature for 3 h and diluted with Et_2O. The solution was washed with 1 M HCl (aq.), H_2O, and brine, and the organic layer was dried over Na_2SO_4. The solvent was removed *in vacuo* and the residue was purified by flash chromatography on silica gel, eluting with DCM/MeOH (95:5) to give compound **10** (290 mg, 79%) as a white solid. ^{1}H NMR (400 MHz, $CDCl_3$) δ = 7.75 (d, *J* = 7 Hz, 2H), 7.52 (s, 2H), 7.38 (dd, *J* = 15 and 8 Hz, 3H), 7.29 (t, *J* = 8 Hz, 3H), 7.12 (dd, *J* = 14 and 7 Hz, 2H), 6.05-5.98 (m, 1H), 4.52-4.40 (m, 3H), 4.21 (t, *J* = 7 Hz, 1H), 3.17 (s, 2H), 1.87-1.75 (m, 2H), 1.50-1.42 (m, 7H); ^{13}C NMR (100 MHz, $CDCl_3$) δ = 175.7, 171.3, 163.2, 156.3, 155.9, 143.8, 143.7, 136.6, 133.8, 128.7, 127.7, 127.0, 126.3, 125.1, 124.9, 119.9, 118.1, 69.1, 68.1, 67.1, 60.4, 53.6, 47.1, 40.5, 36.8, 31.8, 31.7, 29.3, 22.2, 21.6, 21.0, 14.1; HRMS-ESI (*m/z*) $[M+H]^+$ calculated for $C_{30}H_{32}O_6N_5$: 558.23471; found 558.23383.

***N*^{6}-((((2-Azidophenyl)ethane)oxy)carbonyl)-*L*-lysine (MOABK**, **11).** Compound **10** (50 mg, 89.7 *μ*mol) was dissolved in DCM (0.72 mL) and piperidine (0.18 mL) was added at room temperature. The reaction mixture was stirred at room temperature for 1 h and the solvent was removed *in vacuo*. The residue was purified by flash chromatography on silica gel, eluting with DCM/MeOH (1:1) to give compound **11** (20 mg, 67%) as a white solid. ^{1}H NMR (400 MHz, DMSO-d_6) δ = 7.48 (s, 2H), 7.40-7.36 (m, 2H), 7.30-7.20 (m, 3H), 5.79 (dd, *J* = 13 and 6 Hz, 1H), 3.06 (t, *J* = 6 Hz, 1H), 2.91 (t, *J* = 6 Hz, 2H), 1.72-1.65 (m, 1H), 1.57-1.52 (m, 1H), 1.38-1.29 (m, 7H); ^{13}C NMR (100 MHz, DMSO-d_6) δ = 170.3, 155.3, 135.7, 134.1, 128.8, 125.9, 125.2, 118.5, 66.4, 54.0, 30.7, 29.1, 22.4, 21.7; HRMS-ESI (*m/z*) $[M+H]^+$ calculated for $C_{15}H_{22}O_4N_5$: 336.16663; found 336.16758.

Preparation of MPABK. **MPABK**'s synthesis was similar, although the NHS carbonate could not be isolated. Diazotization of commercially-available 4-aminoacetophenone **12** followed by treatment with sodium azide afforded 4-azidoacetophenone **13** in excellent yield. Sodium borohydride smoothly reduced the ketone to alcohol **14**. Alcohol **14** was treated with DSC in the presence of Et_3N in MeCN for 8 h; *N*$^{\alpha}$-Fmoc-Lys-OH was added directly to the reaction mixture to Fmoc-**MOABK 15** in moderate yield. Piperidine cleanly removed the Fmoc group to provide **MPABK 16** in good yield. To enhance solubility for use in cell culture experiments, **16** was dissolved in HCl in dioxane-CH_2Cl_2 and concentrated down to give the hydrochloride salt **17** (**Scheme S3**).

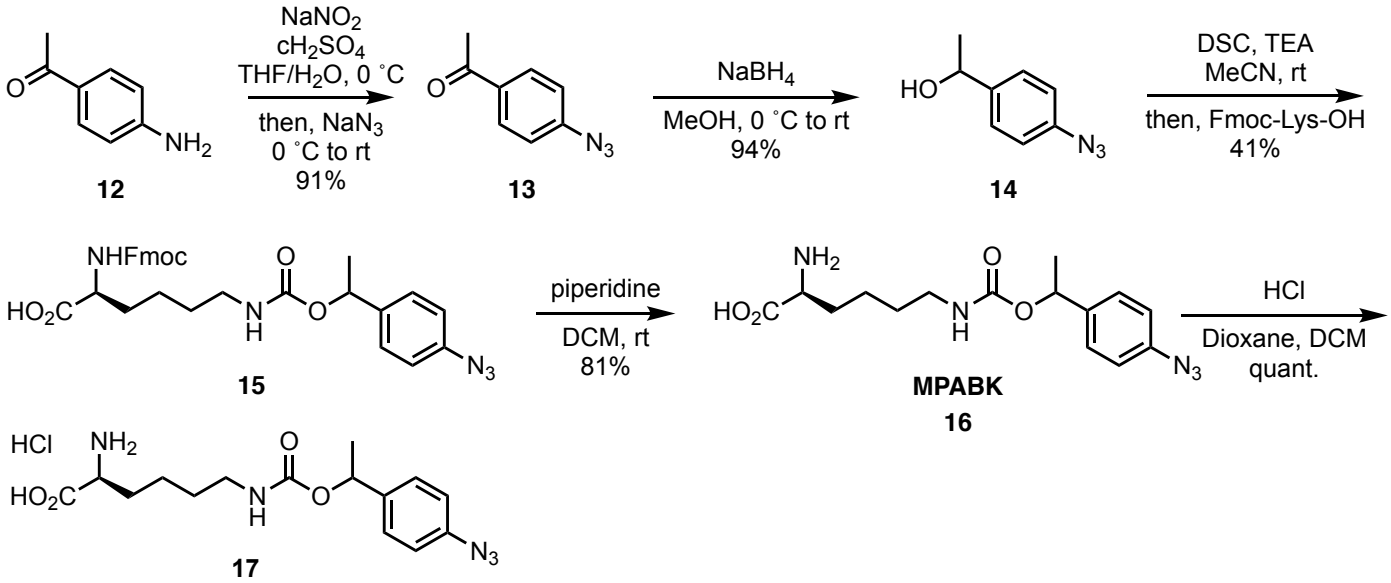

Scheme S3. Synthesis of **MPABK** in 4 steps from 4-aminoacetophenone. The NHS carbonate generated from **14** could not be purified; it was generated *in situ* and treated directly with Fmoc-Lys-OH.

4-Azidoacetophenone (13). 4-Aminoacetophanone (**12**) (1.00 g, 7.40 mmol) was dissolved in THF/H_2O (15/48 mL) and $NaNO_2$ (613 mg, 8.88 mmol) in H_2O (6 mL) was added at 0 ˚C. The reaction mixture was stirred at 0 ˚C for 0.5 h and NaN_3 (577 mg, 8.88 mmol) in H_2O (6 mL) was added. The reaction mixture was stirred at room temperature for 2 h and extracted with DCM. The organic layer was washed with brine and dried over Na_2SO_4. The solvent was removed *in vacuo* and the residue was purified by flash chromatography on silica gel, eluting with hexanes/EtOAc (9:1) to give compound **13** (1.08 g, 91%) as a yellow solid. The analytical data matched reported results.[43]

1-(4-Azidophenyl)ethane-1-ol (14). Compound **13** (1.05 g, 6.52 mmol) was dissolved in MeOH (26 mL) and $NaBH_4$ (246 mg, 6.52 mmol) was added at 0 ˚C over 20 min. The reaction mixture was stirred at room temperature for 1 h and the solvent was removed in vacuo. The residue was resuspended in EtOAc and washed with H_2O and brine. The organic layer was dried over Na_2SO_4 and the solvent was removed in vacuo. The residue was purified by flash chromatography on silica gel, eluting with hexanes/EtOAc (4:1) to give compound **14** (1.00 g, 94%) as a yellow oil. The analytical data matched reported results.[44]

***N*²-(((9*H*-Fluoren-9-yl)methoxy)carbonyl)-*N*⁶-((1-(4-azidophenyl)ethoxy)carbonyl)-*L*-lysine (Fmoc-MPABK, 15).** Compound **14** (70 mg, 0.429 mmol) was dissolved in acetonitrile (4 mL), and TEA (180 μL, 1.3 mmol) and DSC (165 mg, 0.643 mmol) were added at room temperature. The reaction mixture was stirred for 8 h at room temperature and Fmoc-Lys-OH (237 mg, 0.644 mmol) was added. The reaction mixture was stirred at room temperature for 15 h and diluted with DCM. The solution was washed with 1 M HCl aq., H_2O and brine and the organic layer was dried over Na_2SO_4. The solvent was removed in vacuo and the residue was purified by flash chromatography on silica gel, eluting with DCM/MeOH (95:5) to give compound **15** (98 mg, 41%) as a white solid. ^{1}H NMR (400 MHz, $CDCl_3$) δ = 7.76 (d, *J* = 7 Hz, 2H), 7.59 (s, 2H), 7.41-7.30 (m, 6H), 7.00-6.96 (m, 2H), 5.75 (d, *J* = 6 Hz, 1H), 4.50-4.38 (m, 3H), 4.21 (d, *J* = 8 Hz, 1H), 3.16 (s, 2H), 6.961.88-1.75 (m, 2H), 1.53-1.40 (m, 7H); ^{13}C NMR (100 MHz, $CDCl_3$) δ = 176.1, 156.2, 143.8, 143.6, 141.3, 139.6, 139.4, 138.8, 127.7, 127.5, 127.0, 125.1, 119.9, 119.0, 73.2, 72.3, 67.1, 53.6, 47.1, 40.4, 31.7, 29.3, 22.2; HRMS-ESI (*m/z*) $[M+H]^+$ calculated for $C_{30}H_{32}O_6N_5$: 558.23471; found 556.23348. $[M-H]^-$ calculated for $C_{30}H_{30}O_6N_5$: 556.21906; found 556.21942.

***N*⁶-((((4-Azidophenyl)ethane)oxy)carbonyl)-*L*-lysine (MPABK, 16).** Compound **15** (90 mg, 0.162 μmol) was dissolved in DCM (1.3 mL) and piperidine (0.32 mL) was added at room temperature. The reaction mixture was stirred at room temperature for 1.5 h and the solution removed in vacuo. The residue was purified by flash chromatography on silica gel, eluting with DCM/MeOH (1:1) to give compound **16** (44 mg, 81%) as a white solid.

^{1}H NMR (400 MHz, DMSO-d_6) δ = 7.37 (d, J = 8 Hz, 2H), 7.20 (t, J = 8 Hz, 1H), 7.11 (d, J = 8 Hz, 2H), 5.65 (dd, J = 12 and 6 Hz, 1H), 3.06 (t, J = 6 Hz, 1H), 2.92 (t, J = 6 Hz, 2H), 1.68-1.42 (m, 2H), 1.42 (d, J = 6 Hz, 3H), 1.35-1.23 (m, 4H); ^{13}C NMR (126 MHz, DMSO*) δ = 171.8, 156.4, 140.6, 139.3, 128.3, 119.9, 71.5, 67.2, 52.7, 30.4, 29.7, 23.3, 22.5; HRMS-ESI (*m/z*) [M-H]$^-$ calculated for $C_{15}H_{20}O_4N_5$: 334.15098; found 334.15195 [M-H]$^-$ calculated for $C_{15}H_{20}O_4N_5$: 334.15098; found 334.15195. * — this NMR spectrum was obtained in non-deuterated DMSO with a D_2O external standard (in a sealed melting point capillary tube) providing the deuterium signal for locking and shimming. To obtain the hydrochloride salt **17**, a 4 M solution of HCl in 1,4-dioxane (69 μL, 276 μmol) was added to a solution of the product (44 mg, 131 μmol) in dichloromethane (8.0 mL). The reaction mixture was stirred for 5 min and the solvent was removed in vacuo, affording the HCl salt as a yellow solid in quantitative yield (71 mg, 192 mmol). The HCl salt is highly soluble in DMSO (≥ 100 mM) and in aqueous media (≥ 1 mM).

4. NMR Spectra of New Compounds

1H-NMR of Fmoc-**MPABK 15** (500 MHz, CD_3OD):

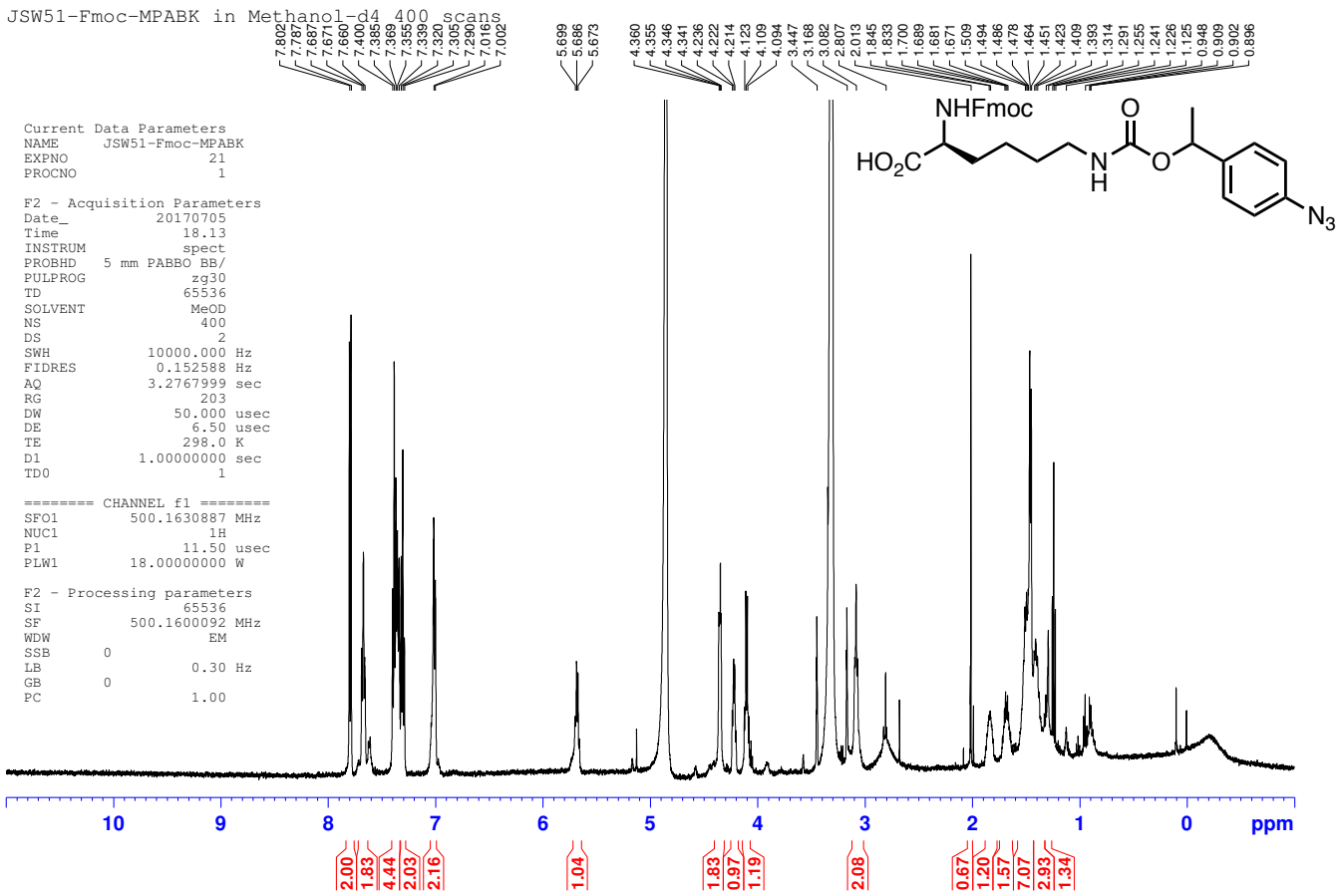

1H-NMR of Fmoc-**MPABK** 15 (500 MHz, $CDCl_3$):

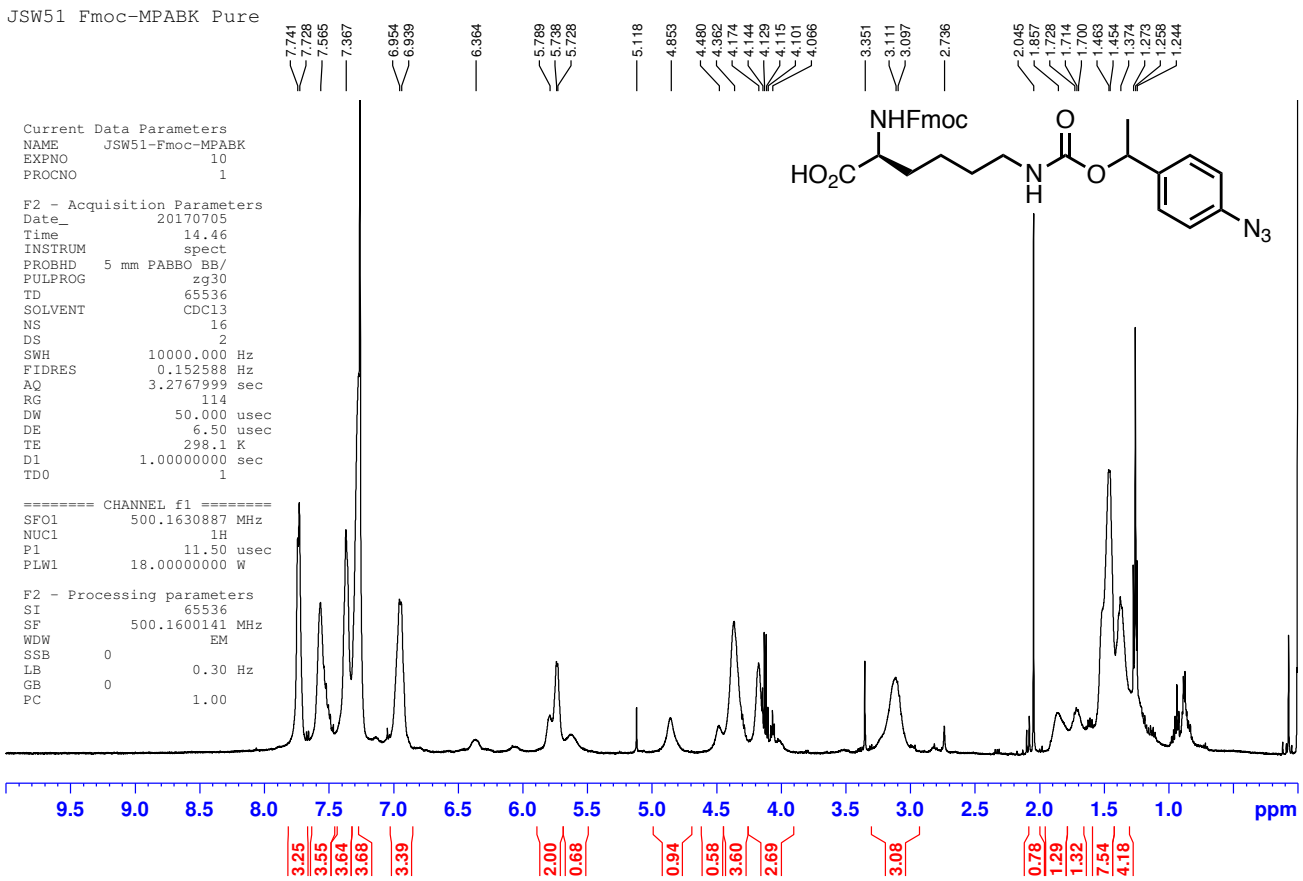

^{13}C-NMR of Fmoc-**MPABK 15** (100 MHz, $CDCl_3$)

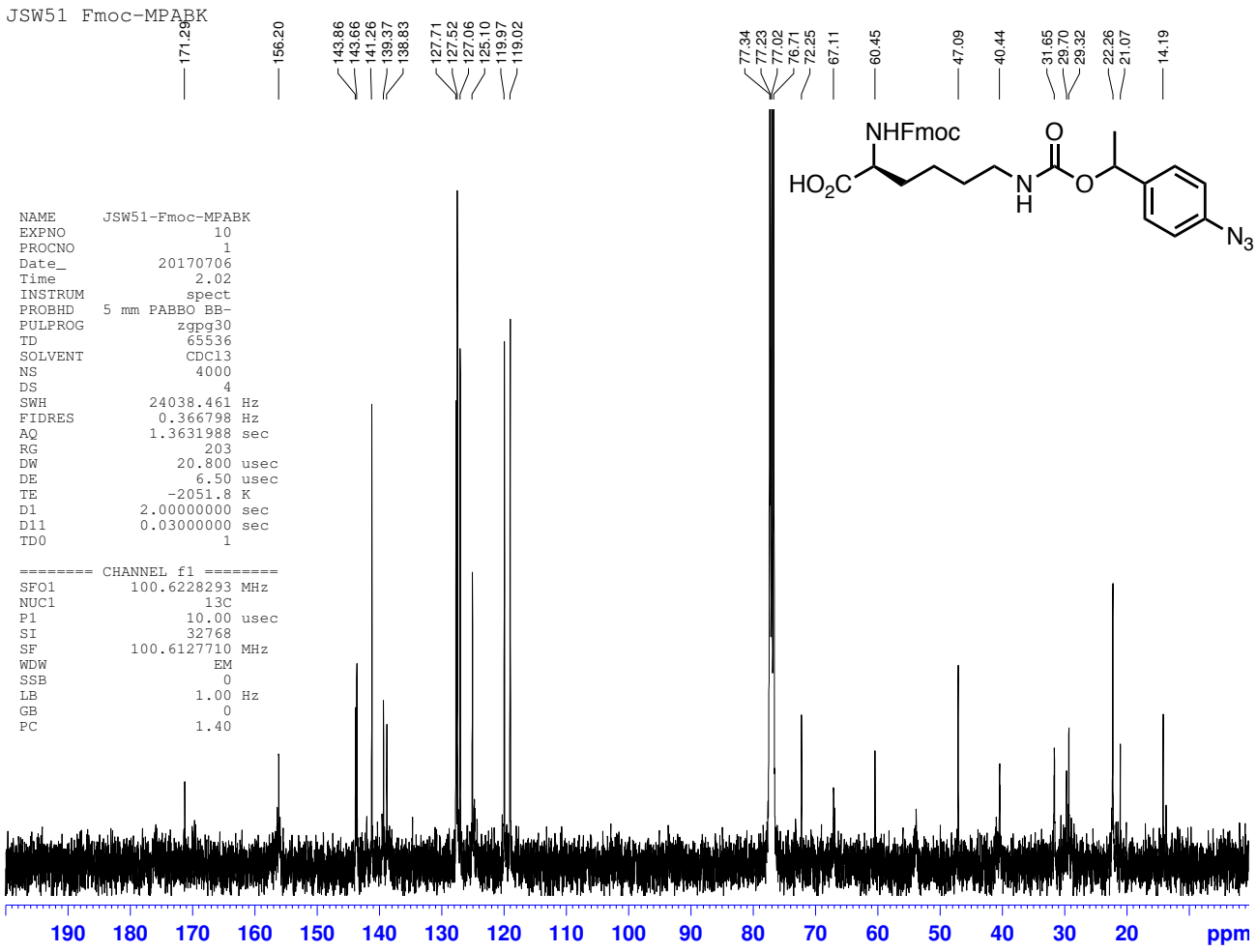

^{1}H-NMR of **MPABK 16** (500 MHz, DMSO-d_6)

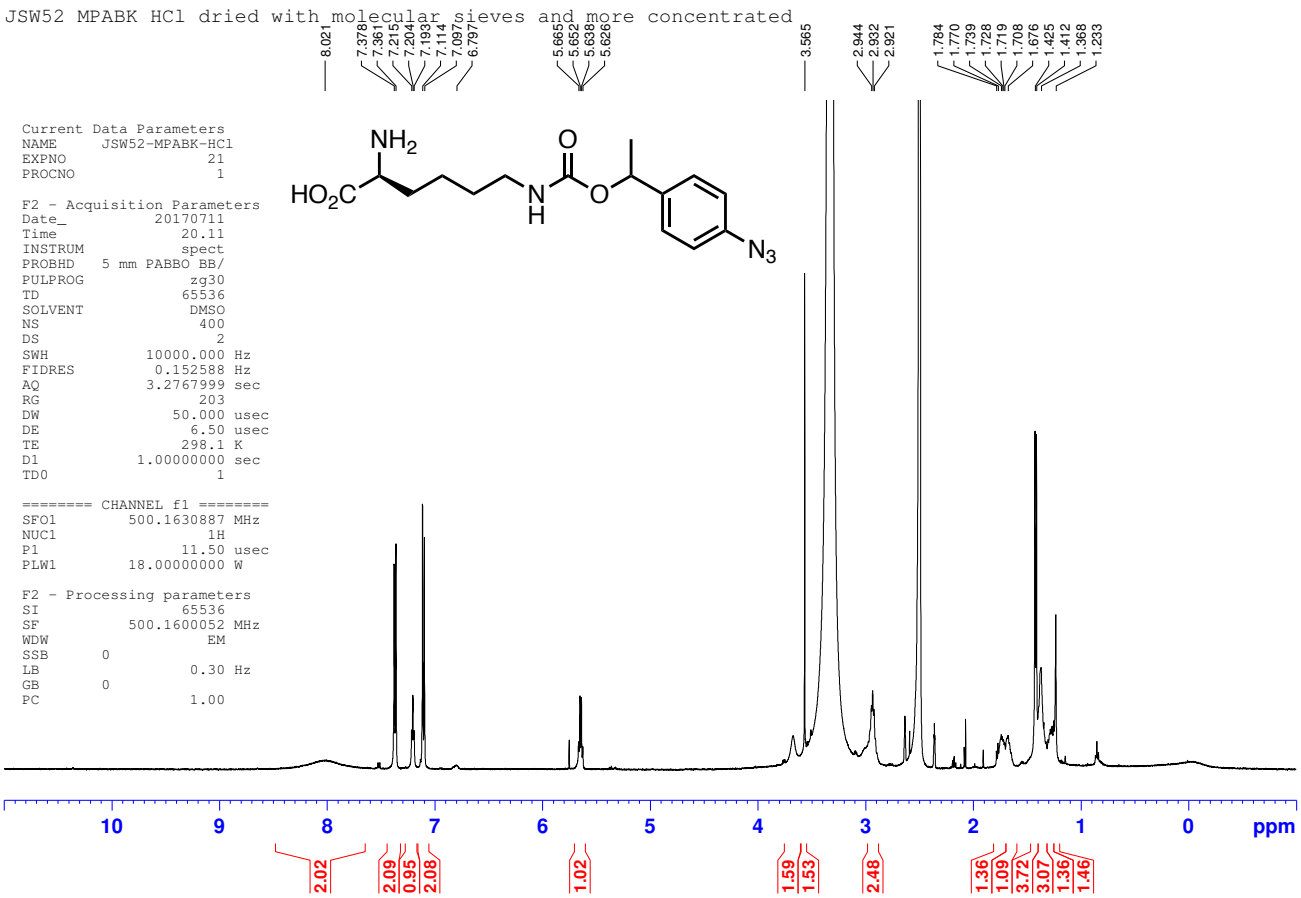

^{13}C-NMR of **MPABK 16** (600 MHz, DMSO)

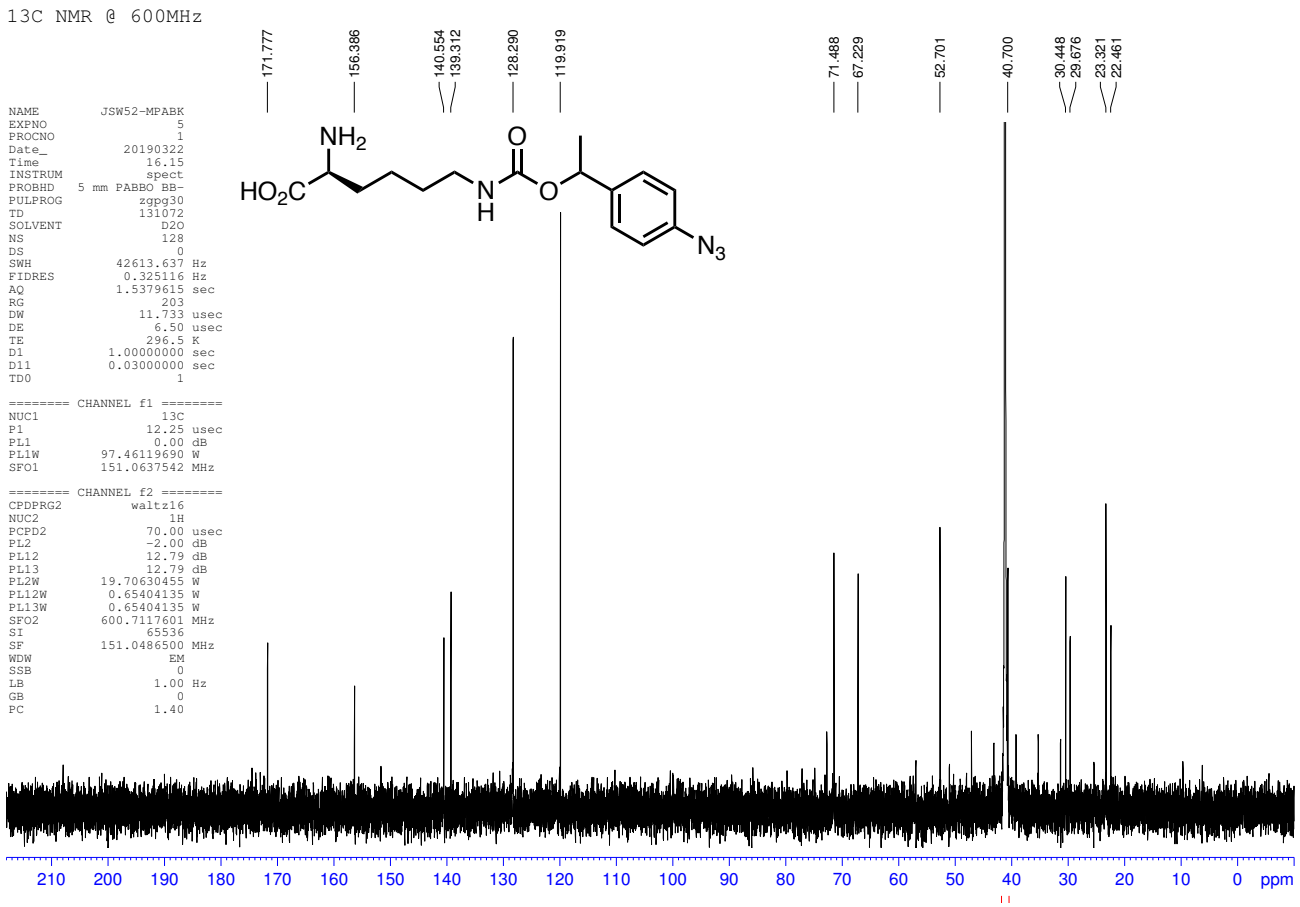

5. Table S2. PylRS mutants used in this work.

	***M. mazei* (*Mm*) numbering**	306	309	348	384
	***M. barkeri* (*Mb*) numbering**	**271**	**274**	**313**	**349**
ID	**Name**				
V1	WTRS (PylRS-WT)	Y	L	C	Y
V12[19]a	BhcKRS	A	M		
V13	OABKRS	A			F
V14	PABKRS		A	A	F
V15[39]			A	S	F
V16				G	F
V17			T		F
V18			T	G	F
V19		A	A		F
V20		A	A	A	F
V21		A		G	F
V22		A		A	F

[a]IPYE quadruple mutant (see “Plasmid construction for mammalian cell applications”).

6. References

[1] J. Luo, Q. Liu, K. Morihiro, A. Deiters, *Nat. Chem.* **2016**, *8*, 1027–1034.
[2] K. L. Kiick, E. Saxon, D. A. Tirrell, C. R. Bertozzi, *Proc. Natl. Acad. Sci. U. S. A.* **2002**, *99*, 19–24.
[3] S. Nehring, N. Budisa, B. Wiltschi, *PLoS One* **2012**, *7*, DOI 10.1371/journal.pone.0031992.
[4] W. Wan, J. M. Tharp, W. R. Liu, *Biochim. Biophys. Acta - Proteins Proteomics* **2014**, *1844*, 1059–1070.
[5] M. J. Schmidt, A. Weber, M. Pott, W. Welte, D. Summerer, *ChemBioChem* **2014**, *15*, 1755–1760.
[6] T. Yanagisawa, M. Kuratani, E. Seki, N. Hino, K. Sakamoto, S. Yokoyama, *Cell Chem. Biol.* **2019**, *26*, 1–14.
[7] T. Yanagisawa, R. Ishii, R. Fukunaga, T. Kobayashi, K. Sakamoto, S. Yokoyama, *Chem. Biol.* **2008**, *15*, 1187–1197.
[8] V. Sharma, Y. Zeng, W. W. Wang, Y. Qiao, Y. Kurra, W. R. Liu, *ChemBioChem* **2018**, *19*, 26–30.
[9] A. Bianco, F. M. Townsley, S. Greiss, K. Lang, J. W. Chin, *Nat. Chem. Biol.* **2012**, *8*, 748–750.
[10] O.-K. Park-Sarge, K. D. Sarge, *Methods Mol. Biol.* **2008**, *464*, 255–265.
[11] M. R. Hunter, N. L. Grimsey, M. Glass, *Sci. Rep.* **2016**, *6*, 1–10.
[12] H. D. Ulrich, *Methods Mol. Biol. SUMO Protoc.* **2009**, *497*, 3–16.
[13] G. Bossis, K. Chmielarska, U. Gärtner, A. Pichler, E. Stieger, F. Melchior, *Methods Enzymol.* **2005**, *398*, 20–32.
[14] V. Sakin, S. M. Richter, H. H. Hsiao, H. Urlaub, F. Melchior, *J. Biol. Chem.* **2015**, *290*, 23589–23602.
[15] R. Mahajan, L. Gerace, F. Melchior, C. Delphin, T. Guan, *J. Cell Biol.* **1998**, *140*, 259–270.
[16] J. Mikolajczyk, M. Drag, M. Békés, J. T. Cao, Z. Ronai, G. S. Salvesen, *J. Biol. Chem.* **2007**, *282*, 26217–26224.
[17] M. Békés, J. Prudden, T. Srikumar, B. Raught, M. N. Boddy, G. S. Salvesen, *J. Biol. Chem.* **2011**, *286*, 10238–10247.
[18] J. Joseph, S. H. Tan, T. S. Karpova, J. G. McNally, M. Dasso, *J. Cell Biol.* **2002**, *156*, 595–602.
[19] J. Luo, R. Uprety, Y. Naro, C. Chou, D. P. Nguyen, J. W. Chin, A. Deiters, *J. Am. Chem. Soc.* **2014**, *136*, 15551–15558.
[20] L. Wang, A. Brock, B. Herberich, P. G. Schultz, *Science* **2001**, *292*, 498–500.
[21] J. Schindelin, I. Arganda-Carreras, E. Frise, V. Kaynig, M. Longair, T. Pietzsch, S. Preibisch, C. Rueden, S. Saalfeld, B. Schmid, J. Y. Tinevez, D. J. White, V. Hartenstein, K. Eliceiri, P. Tomancak, A. Cardona, *Nat. Methods* **2012**, *9*, 676–682.
[22] C. A. Schneider, W. S. Rasband, K. W. Eliceiri, *Nat. Methods* **2012**, *9*, 671–675.
[23] H. Engelke, C. Chou, R. Uprety, P. Jess, A. Deiters, *ACS Synth. Biol.* **2014**, *3*, 731–736.
[24] M. V. Shapovalov, R. L. Dunbrack, *Structure* **2011**, *19*, 844–858.
[25] E. F. Pettersen, T. D. Goddard, C. C. Huang, G. S. Couch, D. M. Greenblatt, E. C. Meng, T. E. Ferrin, *J. Comput. Chem.* **2004**, *25*, 1605–12.
[26] J. Wang, W. Wang, P. A. Kollman, D. A. Case, *J. Mol. Graph. Model.* **2006**, *25*, 247–260.
[27] O. Trott, A. J. Olson, *J. Comput. Chem.* **2010**, *31*, 455–461.
[28] M. F. Sanner, A. J. Olson, J. Spehner, *Biopolymers* **1996**, *38*, 305–320.
[29] Y. Nakayama, I. S. Mian, T. Kohwi-Shigematsu, T. Ogawa, *Cell Cycle* **2005**, *4*, 1099–1106.
[30] A. Šali, T. L. Blundell, *J. Mol. Biol.* **1993**, *234*, 779–815.
[31] A. Sali, M.-Y. Shen, *Protein Sci.* **2006**, 2507–2524.
[32] D. G. Gibson, L. Young, R.-Y. Chuang, J. C. Venter, C. A. Hutchison III, H. O. Smith, *Nat. Methods* **2009**, *6*, 343.
[33] T. Suzuki, C. Miller, L. T. Guo, J. M. L. Ho, D. I. Bryson, Y. S. Wang, D. R. Liu, D. Söll, *Nat. Chem. Biol.* **2017**, *13*, 1261–1266.
[34] D. I. Bryson, C. Fan, L. T. Guo, C. Miller, D. Söll, D. R. Liu, *Nat. Chem. Biol.* **2017**, *13*, 1253–1260.
[35] A. Chatterjee, H. Xiao, M. Bollong, H.-W. Ai, P. G. Schultz, *Proc. Natl. Acad. Sci. U. S. A.* **2013**, *110*, 11803–11808.
[36] W. C. Still, M. Kahn, A. Mitra, *J. Org. Chem.* **1978**, *43*, 2923–2925.
[37] H. E. Gottlieb, V. Kotlyar, A. Nudelman, *J. Org. Chem.* **1997**, *62*, 7512–7515.
[38] H. Saneyoshi, T. Ochikubo, T. Mashimo, K. Hatano, Y. Ito, H. Abe, *Org. Lett.* **2014**, *16*, 30–33.
[39] Y. Ge, X. Fan, P. R. Chen, *Chem. Sci.* **2016**, *7*, 7055–7060.

[40] W.-Y. Lu, X.-W. Sun, C. Zhu, J.-H. Xu, G.-Q. Lin, *Tetrahedron* **2010**, *66*, 750–757.
[41] C. J. Smith, C. D. Smith, N. Nikbin, S. V Ley, I. R. Baxendale, *Org. Biomol. Chem.* **2011**, *9*, 1927–1937.
[42] P. Molina, M. Alajarin, A. Vidal, *J. Org. Chem.* **1993**, *58*, 1687–1695.
[43] Y. Li, L.-X. Gao, F.-S. Han, *Chem. A Eur. J.* **2010**, *16*, 7969–7972.
[44] M. R. Maddani, S. K. Moorthy, K. R. Prabhu, *Tetrahedron* **2010**, *66*, 329–333.